

The search for strongly decaying exotic matter

R.S. Longacre^a

^aBrookhaven National Laboratory, Upton, NY 11973, USA

Abstract

In this paper we explore the possibility of detecting strongly decaying exotic states. The dibaryon(2.15) $J^P = 2^+$ state which decays into $d \pi$ is the example we use in this report.

1 Introduction

At the STAR experiment we can collect hundreds of million ultra-relativistic heavy ion collisions. Light nuclei and anti-nuclei emerge from these collisions during the last stage of the collision process. The quantum wave functions of the constituent nucleons or anti-nucleons, if close enough in momentum and coordinate space, will overlap to produce composite systems. The production rate for the systems with baryon or anti-baryon B is proportional to the baryon or anti-baryon density in momentum and coordinate space, raised to the power |B|, and therefore exhibits exponential behavior as a function of |B|. Figure 1 shows the exponential[1] invariant yields versus baryon number in $\sqrt{s_{NN}}=200$ GeV central Au+Au collisions. Empirically, the production rate reduces by a factor of $1.1 \times 10^3 (1.6 \times 10^3)$ for each additional nucleon (anti-nucleon) added. The measurement of hundreds of million of events make it possible to probe up to a scale of five in baryon number. The baryon four data points come from a STAR measurement published in Ref.[2]. It should be noted that there are no baryon five nuclear fragments that live long enough or decay weakly such that they would have a displaced vertex[2].

The paper is organized in the following manner:

Sec. 1 explores nuclear states that have been measured.

Sec. 2 explores the possibility of detecting strongly decaying exotic states. The dibaryon(2.15) $J^P = 2^+$ state which decays into $d \pi$ is considered.

2 Exotic States through strong decay.

In the above section the states decayed by the weak interaction. The possibility of detecting strongly decaying exotic states is considered using the dibaryon(2.15) $J^P = 2^+$ state which decays into $d \pi$ as an example. In the QGP(Quark Gluon Plasma) six quarks or anti-quarks could come together to form a deuteron or anti-deuteron. However such states are loosely bound and easily destroyed in the hadronic phase. The cross section for $d \pi$ scattering is 240 mb. This implies that the deuteron can only be formed in the final freeze-out of the

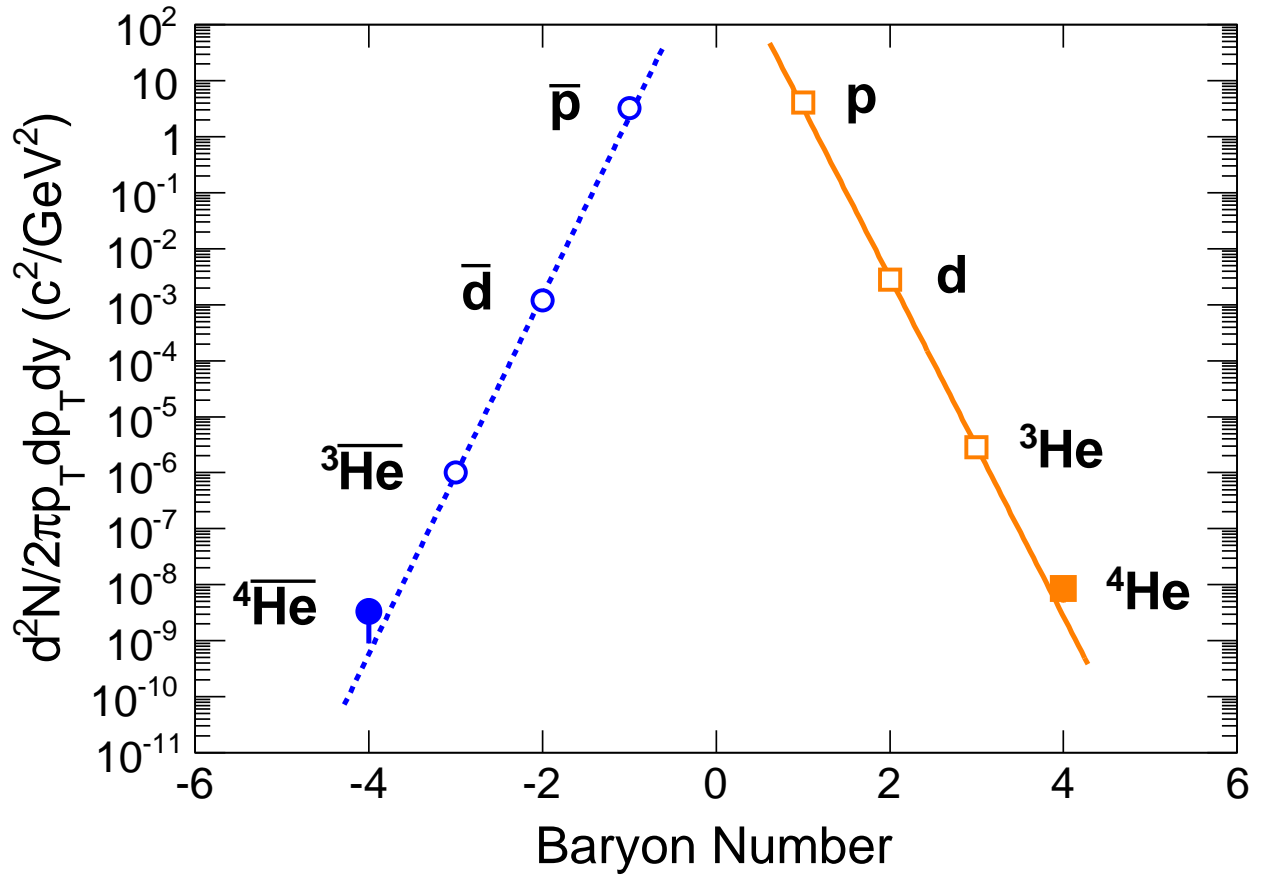


Figure 1: Differential invariant yields as a function of baryon number B , evaluated at $p_T/|B| = 0.875$ GeV/c, in central $\sqrt{s_{NN}}=200$ GeV Au+Au collisions. Yields for tritons ${}^3\text{H}$ (anti-tritons ${}^3\overline{\text{H}}$) lie close to the position for ${}^3\text{He}$ and ${}^3\overline{\text{He}}$. The lines represent fits with the exponential formula $\propto e^{-r|B|}$ for positive and negative particles separately, where r is the production reduction factor.

hadronic system. At the time of freeze-out many hadrons scatter and coalesce into compound or excited states(see Figure 2).

The dibaryon state interacts in three two-body scattering channels. Its mass is 2.15 GeV and has a strong interaction resonance decay width of 100 MeV. It interacts in the NN d-wave spin anti-aligned[3], $d\pi$ p-wave spin aligned[4], and ΔN s-wave spin aligned[5]. The dibaryon system mainly resonates in the s-wave ΔN mode with a pion rotating in a p-wave about a spin aligned NN system which forms a isospin singlet. The pion moves back and forth forming Δ states with one nucleon and then the other(see Figure 3). All three isospin states of the pion can be achieved in this resonance. Thus we can have $\pi^+ d$, $\pi^0 d$, and $\pi^- d$ states. If the pion is absorbed by any of the nucleons it under goes a spin flip producing a d-wave NN system. The resonance decays into NN , πd , or πNN . In a meson system an analogous resonance is formed where a pion is orbiting in a p-wave about a $K\bar{K}$ in a s-wave[6](see Figure 4). Both systems have a similar lifetime or width of $\sim .100$ GeV.

In order to predict the rate for dibaryon production we turn to a Monte Carlo heavy ion event generator[7]. This generator was a cradle to grave going from initial partons to final state hadrons. Figure 5 shows the time line in the center-of-mass frame for partons, then pre-hadrons and final hadrons. What is happening in the early times of the collision is of no importance for dibaryon formation, while the conditions of the hadrons at later times will determine the dibaryon production. For $\sqrt{s_{NN}}=200$ GeV central Au+Au collisions the spectrum is well measured. Therefore we can start the Monte Carlo at the intermediate times with a fireball of excited hadrons and let it evolve to the final state.

We start with an expanding cylinder of radius 10.0 Fermi filled with excited hadrons with density and p_t distribution that reproduces the $\sqrt{s_{NN}}=200$ GeV central Au+Au collisions. Figure 6 gives the measured Au+Au spectrum which we will tune for. Mesons in the fireball cascade include π , K , ρ , ω , a_1 , η , η' , ϕ , K^* , $K^*(1420)$, $f_0(975)$, $a_0(980)$, $f_2(1270)$, $a_2(1320)$, $h_1(1170)$, $\rho(1700)$, $f_2(1800)$, $b_1(1235)$ and $f_2(1525)$. The cross section for $\pi\pi$ and πK was determined from S-matrix phase shifts, while for $K\bar{K}$ we used the production of ϕ , $f_0(975)$, $a_0(980)$, $f_2(1270)$, $a_2(1320)$, and $f_2(1525)$ (see Figure 7). For $\rho\pi$ cross sections we used the production of $h_1(1170)$, $a_1(1260)$, and $a_2(1320)$, while for $K^*\pi$ we used the production of $K^*(1420)$. For $a_1\pi$ we used $\rho(1700)$ and $f_2(1800)$ (see Figure 8). Finally for $\omega\pi$ we used $b_1(1235)$ and $\eta\pi$ we used $a_0(980)$ and $a_2(1320)$. For all other meson meson cross section we used the additive quark model. The particles produced from such scatterings were determined by a multi-pomeron chain model using a Field-Feymann algorithm(see Figure 9).

Since we are detecting baryons and anti-baryons the NN , $N\pi$, NK , and ΔN cross section and scattering ratios are obtained from data and extracted S-matrix amplitudes(see Figure 10). All other cross sections for baryon meson and baryon baryon systems we use the additive quark model(see Figure 11). The particles produced from such scatterings are determined by a multi-pomeron chain model using a Field-Feymann algorithm. For baryon(B) anti-baryon(\bar{B}) scattering and cross section, data is used for $N\bar{N}$ annihilation and elastic scattering. For annihilation yields, we use a flavor consistent meson meson multi-pomeron chain model. For the rest of the yield a $B\bar{B}$ multi-pomeron chain model is used. The elastic scattering obtained by this method is close to the data for the $N\bar{N}$ system.

At the time of freeze-out
many hadrons scatter and
coalesce into compound or
excited states.

$$\pi \pi \rightarrow \rho$$

$$\pi \rho \rightarrow a_1$$

$$\pi K \rightarrow K^*$$

$$\pi N \rightarrow \Delta$$

$$\pi d \rightarrow N \Delta$$

$$\pi p n \rightarrow \pi d$$

Figure 2: Above are a few of the compound or excited states that will form during the last stage of hadronic freeze-out.

Spin aligned s-wave $N \Delta$ coalescence

Form a dibaryon spin aligned $N N$
system in a s-wave with a π in
a p-wave orbiting around like
an atomic system

$J^P = 2^+$ mass = 2.15 GeV width = .100 GeV

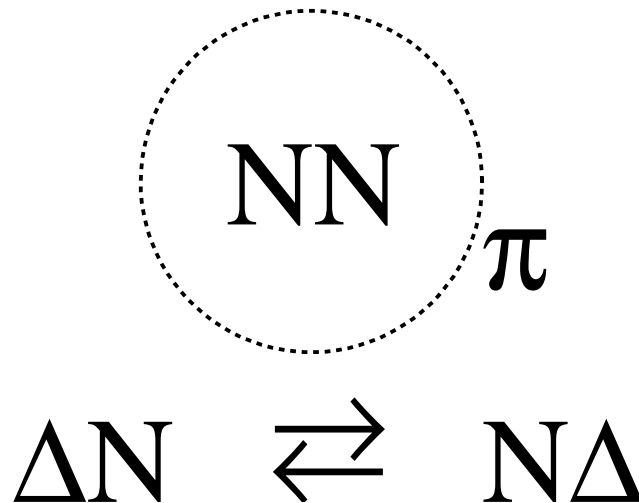


Figure 3: The dibaryon system mainly resonates in the s-wave ΔN mode with a pion rotating in a p-wave about a spin aligned $N N$ system which forms a isospin singlet. The pion moves back and forth forming Δ states with one nucleon and then the other.

a meson p-wave π orbiting atomic
system can also be formed

(Phys Rev D 42 (1990) 874)

$J^P = 1^+$ mass = 1.42 GeV width = .100 GeV

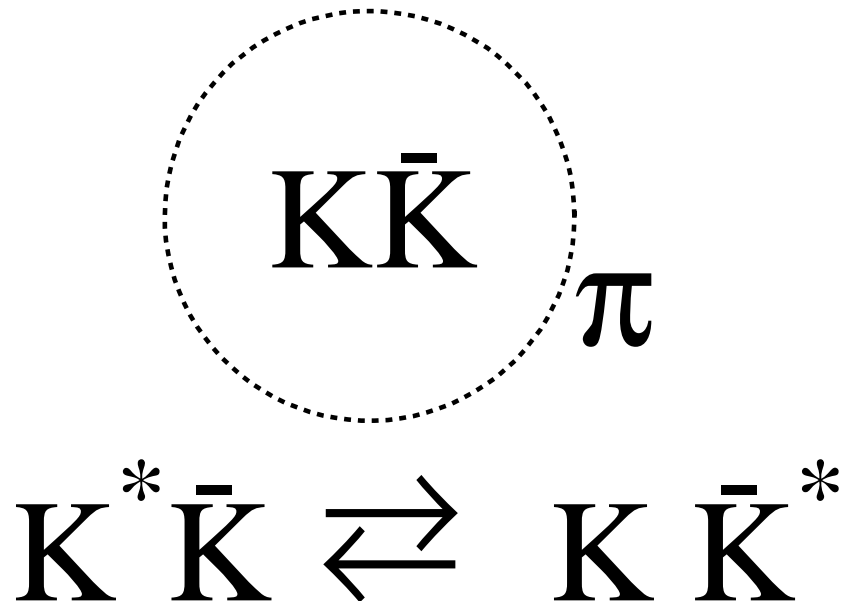


Figure 4: The meson system mainly resonates in the s-wave $K^* \bar{K}$ and $K \bar{K}^*$ mode with a pion rotating in a p-wave about a $K \bar{K}$ system which forms a isospin triplet. The pion moves back and forth forming K^* and \bar{K}^* states with one K or \bar{K} .

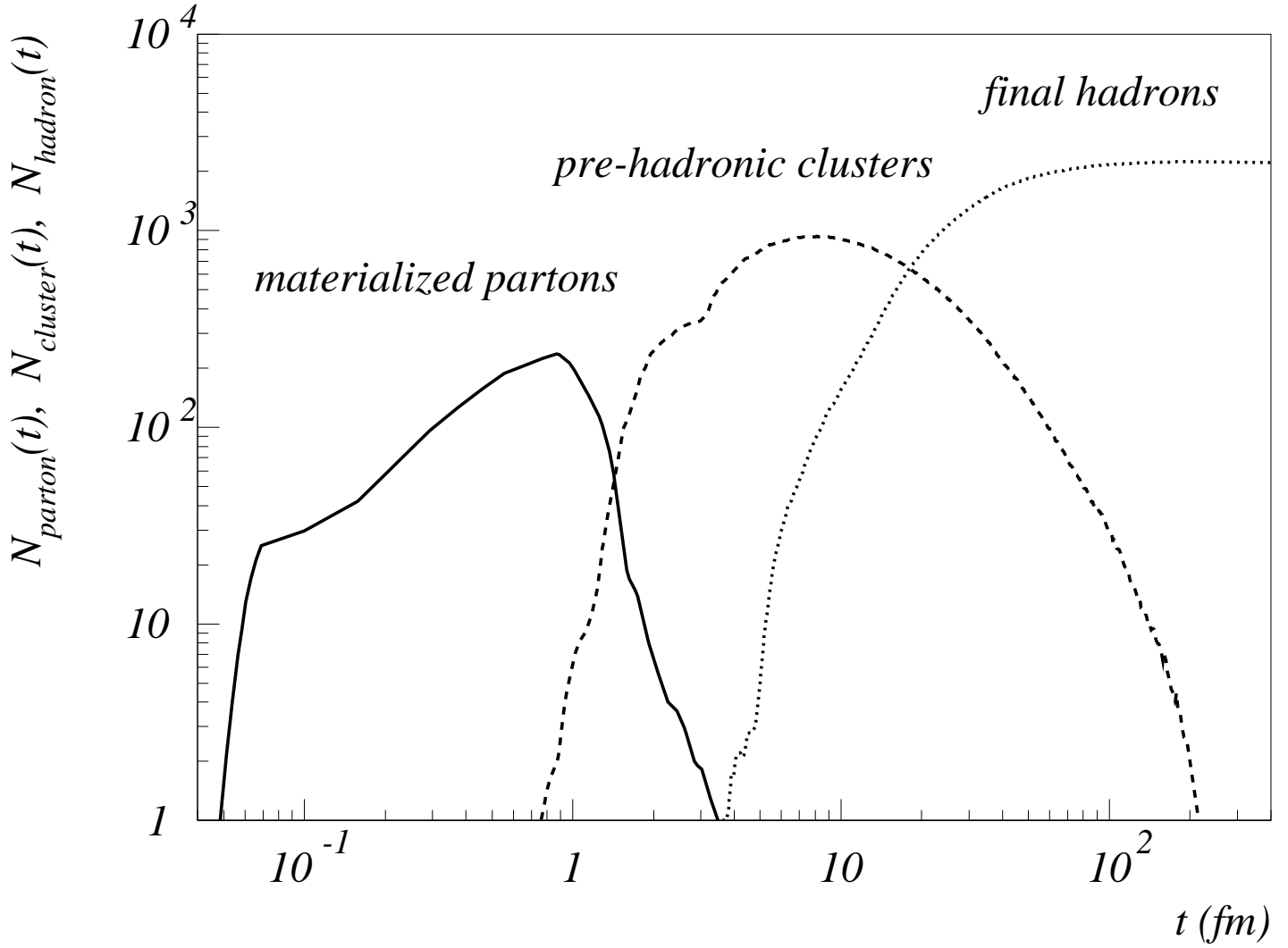


Figure 5: Time evolution of the total numbers of produced partons N_p , pre-hadronic clusters N_c , and hadrons N_h during Au + Au collisions. The time refers to the center-of-mass frame of the colliding nuclei.

STAR has measured Au Au spectra for
central collisions at $\sqrt{s_{\text{NN}}} = 200 \text{ GeV}$

for $P_t > 0.2 \text{ GeV}/c$ and $|\eta| < 1.0$

$$\pi \rightarrow 1128$$

$$K \rightarrow 214$$

$$p \rightarrow 67$$

$$\bar{p} \rightarrow 50$$

Our goal is to match the numbers and
the P_t spectra that STAR has measured

Figure 6: The measured Au+Au spectrum which we will tune for.

Cross section from phase shifts S-matrix

$$\begin{array}{ll}
 \pi \pi \rightarrow \pi \pi & \pi \pi \rightarrow K \bar{K} \\
 \pi \pi \rightarrow \eta \eta & \pi K \rightarrow K \pi \\
 \pi K \rightarrow K \pi \pi & \pi K \rightarrow K \pi \pi \pi
 \end{array}$$

$$\begin{array}{l}
 K \bar{K} \text{ assuming } f_0(975) \text{ } a_0(980) \\
 \phi(1020) \text{ } f_2(1270) \text{ } a_2(1320) \text{ } f_2(1525)
 \end{array}$$

$$\begin{array}{ll}
 K \bar{K} \rightarrow K \bar{K} & K \bar{K} \rightarrow \pi \pi \\
 K \bar{K} \rightarrow \eta \eta & K \bar{K} \rightarrow \eta \pi \\
 & K \bar{K} \rightarrow \rho \pi
 \end{array}$$

Figure 7: Cross sections for $\pi\pi$, πK , and $K\bar{K}$.

$\rho \pi$ assuming $h_1(1170)$ $a_1(1260)$ $a_2(1320)$

$$\rho \pi \rightarrow \rho \pi \quad \rho \pi \rightarrow K \bar{K}$$

$$\rho \pi \rightarrow \eta \pi$$

$K^* \pi$ assuming $K^*(1420)$

$$K^* \pi \rightarrow K^* \pi \quad K^* \pi \rightarrow K \pi$$

$a_1 \pi$ assuming $\rho(1700)$ $f_2(1800)$

$$a_1 \pi \rightarrow a_1 \pi \quad a_1 \pi \rightarrow \pi \pi$$

Figure 8: Cross sections for $\rho\pi$, $K^*\pi$, and $a_1\pi$.

$\omega \pi$ assuming $b_1(1235)$

$$\omega \pi \rightarrow \omega \pi \quad \omega \pi \rightarrow K \bar{K} \pi$$

$\eta \pi$ assuming $a_0(980)$ $a_2(1320)$

$$\eta \pi \rightarrow \eta \pi \quad \eta \pi \rightarrow K \bar{K}$$

Cross Section for other meson meson systems we use the additive quark model.

For production a multi-pomeron chain model is used with a Field - Feymann algorithm.

Figure 9: Cross sections for $\omega\pi$, $\eta\pi$, and others.

Cross Section from Data and S-matrix

$$\begin{array}{lll}
 N\pi \rightarrow N\pi & N\pi \rightarrow \Delta & N\pi \rightarrow \Delta\pi \\
 N\pi \rightarrow N\rho & N\pi \rightarrow N\eta & N\pi \rightarrow \Lambda K \\
 N\pi \rightarrow \Sigma K & NK \rightarrow NK & NK \rightarrow \Delta K \\
 NK \rightarrow NK\pi & N\bar{K} \rightarrow N\bar{K} & N\bar{K} \rightarrow \Lambda\pi \\
 N\bar{K} \rightarrow \Lambda\pi\pi & N\bar{K} \rightarrow \Sigma\pi & N\bar{K} \rightarrow \Sigma\pi\pi \\
 N\bar{K} \rightarrow N\bar{K}\pi & N\bar{K} \rightarrow \Delta\bar{K} & N\bar{K} \rightarrow \Xi K \\
 NN \rightarrow NN & NN \rightarrow \Delta N & NN \rightarrow \Delta\Delta \\
 NN \rightarrow NN\pi & \Delta N \rightarrow NN & \Delta N \rightarrow \Delta N
 \end{array}$$

Figure 10: Cross sections for $N\pi$, NK , NN and others.

Additive Quark Model

Particle	AQM factor
meson light quarks π	4.2
baryon light quarks N	6.3
meson one strange K	3.2
baryon one strange Λ	5.3
meson two strange ϕ	2.5
baryon two strange Ξ	4.3
baryon three strange Ω	3.3

Particle(1) on Particle(2)

$$\sigma = \text{AQM}_1 \times \text{AQM}_2 \text{ mb}$$

Figure 11: The additive quark model calculates the cross section for the scattering of any two particles based on a product of geometric factors.

The annihilation threshold effect is scaled to other $B\bar{B}$ scatterings using the $N\bar{N}$ ratios obtained in the above algorithm.

We need to add the production of d's into the Monte Carlo code. Let us assume that the formation of the $J^P = 2^+$ dibaryon state is the driving source of d's. We fit the d-wave NN elastic scattering[3], p-wave $d\pi$ elastic scattering[4], and p-wave $d\pi$ to d-wave NN [4]. A three channel K-matrix was used to form a S-matrix, where the channels are d-wave NN , p-wave $d\pi$, and s-wave ΔN data. We are able to fit the above data if we use one K-matrix pole to generate the dibaryon 2.15 GeV state plus a far away pole and a flat none factorable background. Figure 12 shows the fit to elastic NN scattering amplitude. Figure 13 shows the fit to $d\pi$ elastic scattering, while Figure 14 is the connection between NN going to $d\pi$.

The cross sections for $NN \rightarrow \pi d$, $\Delta N \rightarrow \pi d$, $\pi d \rightarrow \Delta N$ and NN where added to the hadron cascade part of the code. When we consider the known cross sections for NN and ΔN , the yield for charge pairs of $d\pi$ can be calculated and is plotted in Figure 15. In our hadron cascade these scatterings are the only source of d's. The production of d's and anti-d's is close to the values measured in Figure 1. The value of d's in the cascade would be much larger than the measured value except d's are destroyed by interacting with pions. Figure 16 show the large $d\pi$ cross section of ~ 250 mb. About 3/4 of these scattering remove the d's from the cascade.

We achieve the yield and spectrum for Au+Au $\sqrt{s_{NN}}=200$ GeV central collisions by adjusting the excited hadrons in our cylinder of radius 10.0 Fermi. We generate enough events at $\sqrt{s_{NN}}=200$ GeV central Au+Au collisions in order to obtain 1 million d or \bar{d} events in the STAR acceptance. Out of the 1 million events there were 230,000 pairs of either $d\pi$ or $\bar{d}\pi$ which decayed in the STAR acceptance. The effective mass distribution of these pairs are plotted as solid points in Figure 17.

In order to obtain the mass spectrum from the data, We need to determined the uncorrelated background of either d or \bar{d} paired with a charge particle in a average event. For each of the 1 million events we can pair up either the d or \bar{d} with all charge particles(which then is assumed to be a pion) in that event and plot the total number of pairs as a function of effective mass. From this pair spectrum we then subtract the average uncorrelated spectrum times the number of events. We can determine this average uncorrelated spectrum by mixed event methods taking the same d and \bar{d} paired with the charged particles from other events. The subtracted effective mass spectrum is the open points of Figure 17. We see that we have recovered the mass spectrum.

3 Summary and Discussion

In the first section of this manuscript we consider baryons and anti-baryons up to a baryon number five. These states decayed by the weak interaction. The exotic states that decay strongly is considered in the second section. In order to develop methods for such research we consider a dibaryon(2.15) $J^P = 2^+$ state which decays into $d\pi$.

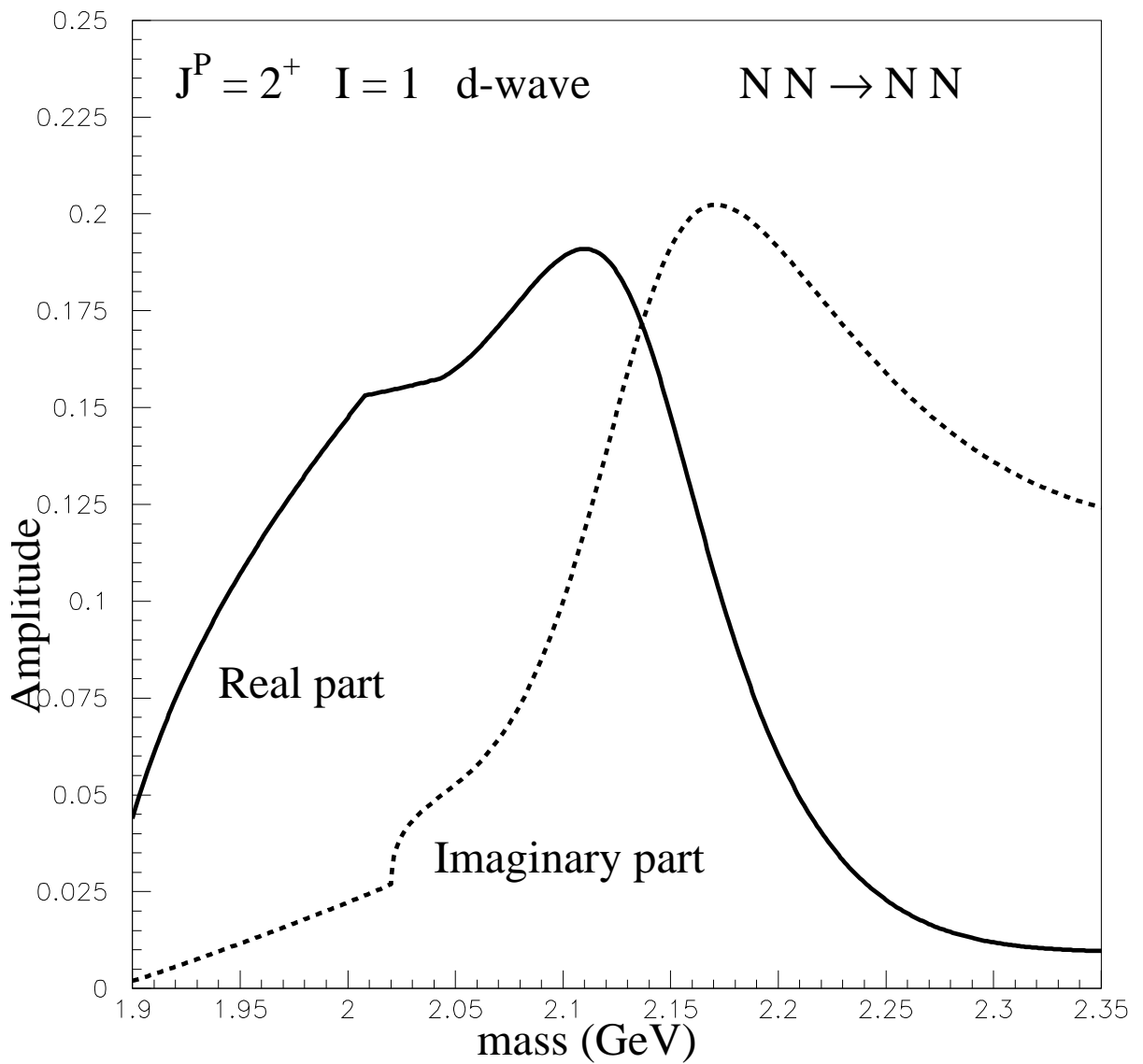


Figure 12: The real and imaginary parts of the elastic scattering T-matrix amplitude for $NN \rightarrow NN$ as a function of mass in GeV.

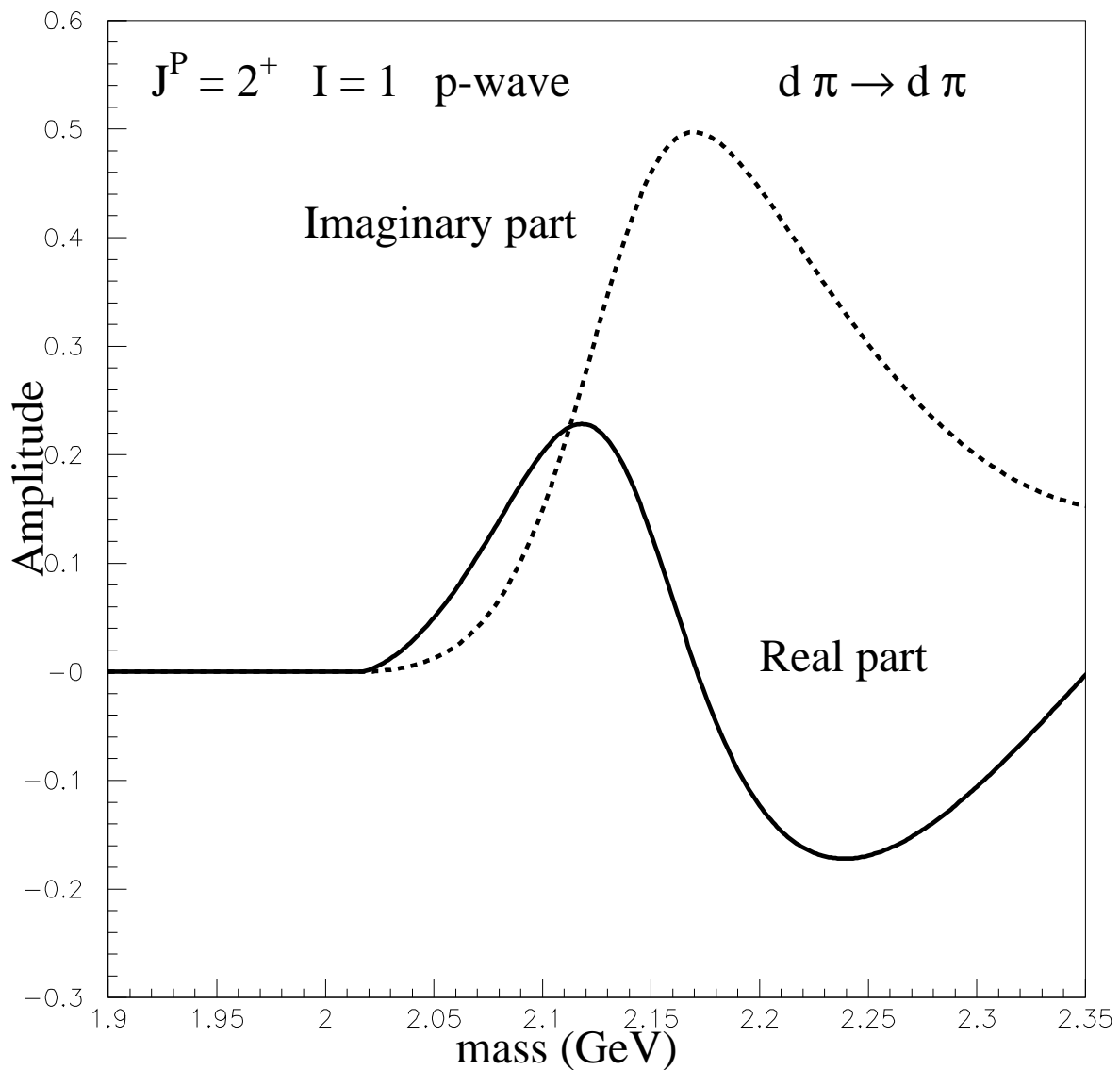


Figure 13: The real and imaginary parts of the elastic scattering T-matrix amplitude for $d\pi \rightarrow d\pi$ as a function of mass in GeV.

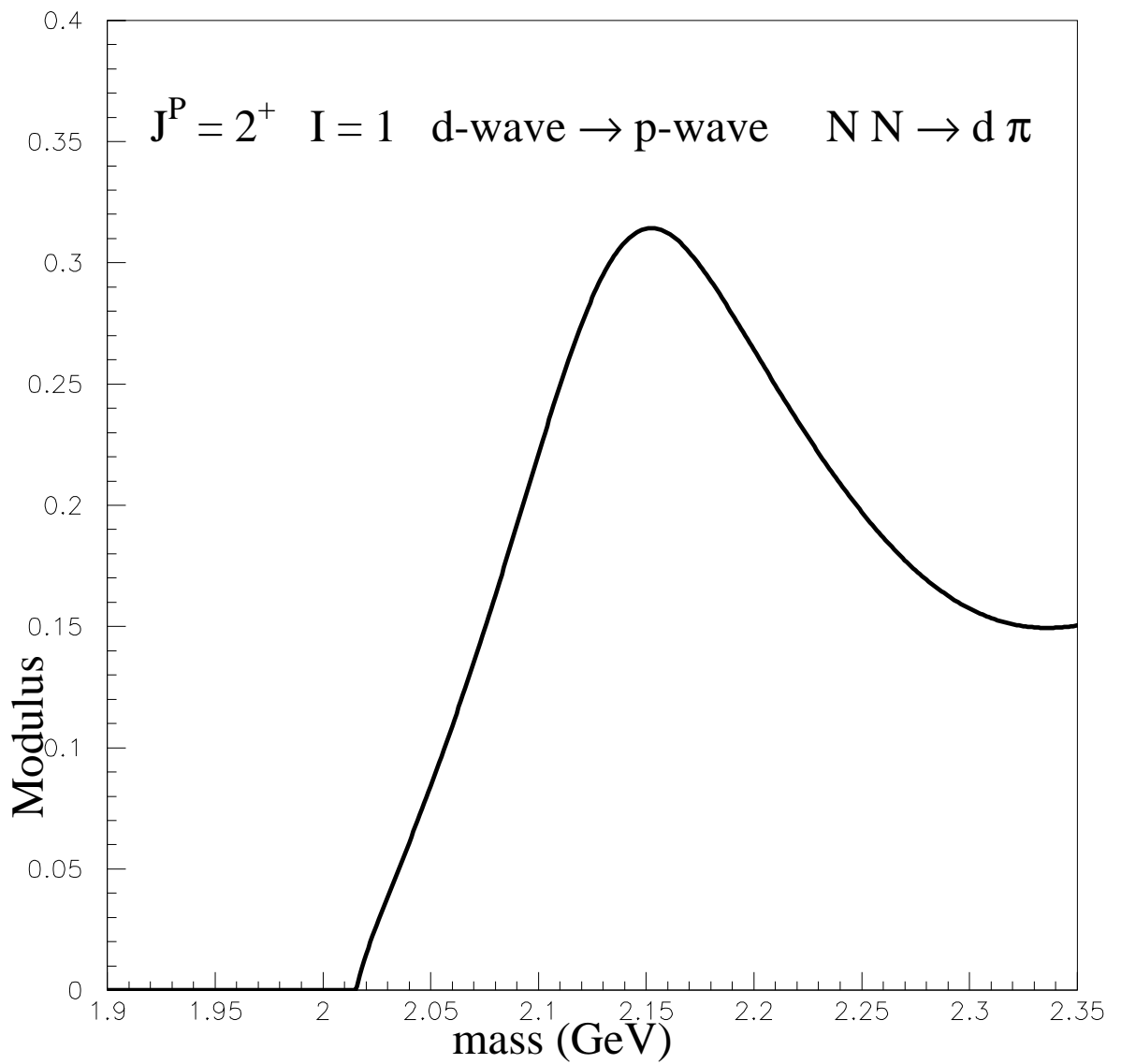


Figure 14: The modulus of the inelastic scattering T-matrix amplitude for $NN \rightarrow d\pi$ as a function of mass in GeV.

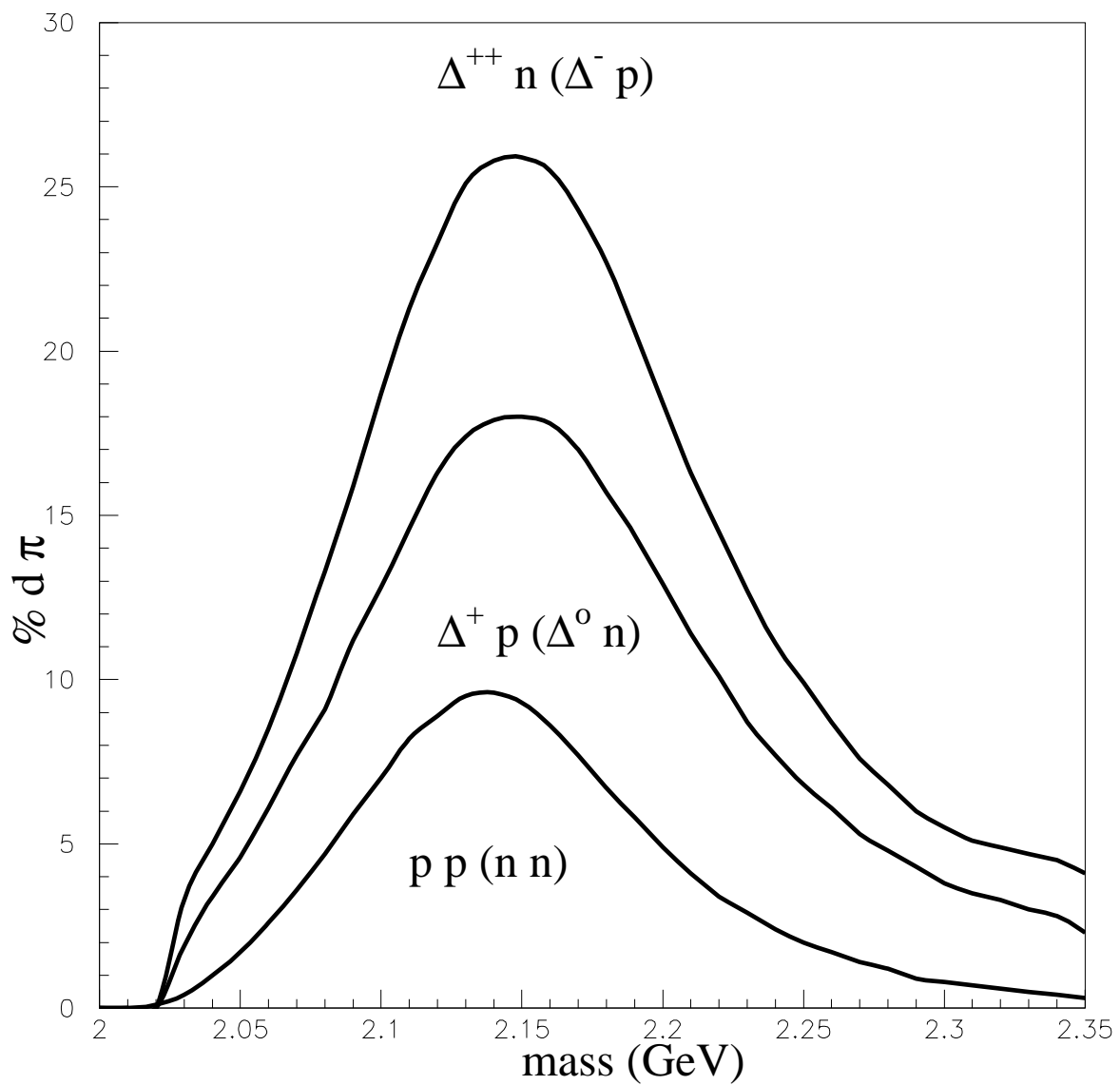


Figure 15: The percentage of $d\pi$ charge pairs produced in NN and ΔN scattering as a function of mass in GeV.

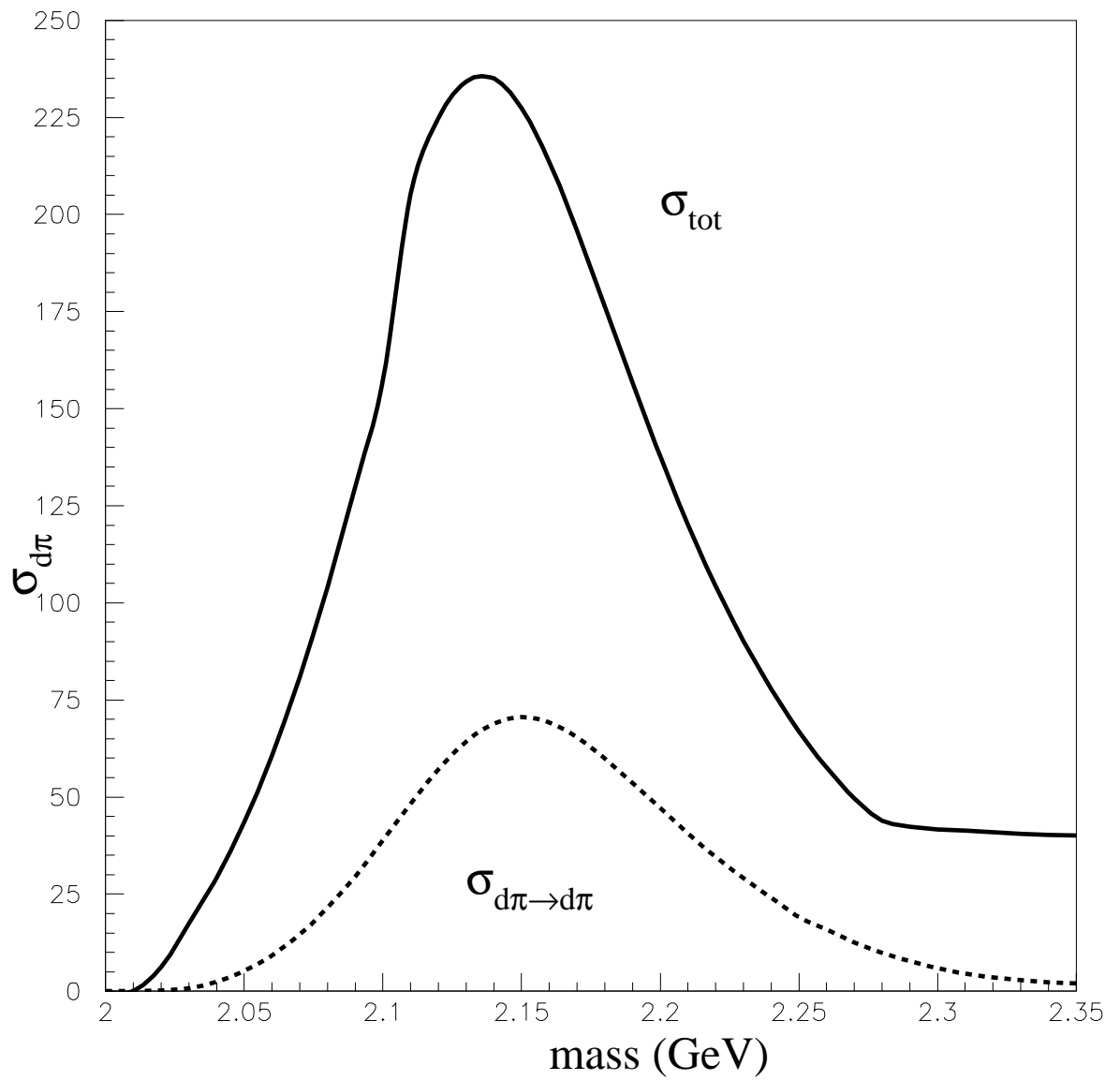


Figure 16: The $d\pi$ total and elastic cross section in millibarns(mb) as a function of mass in GeV.

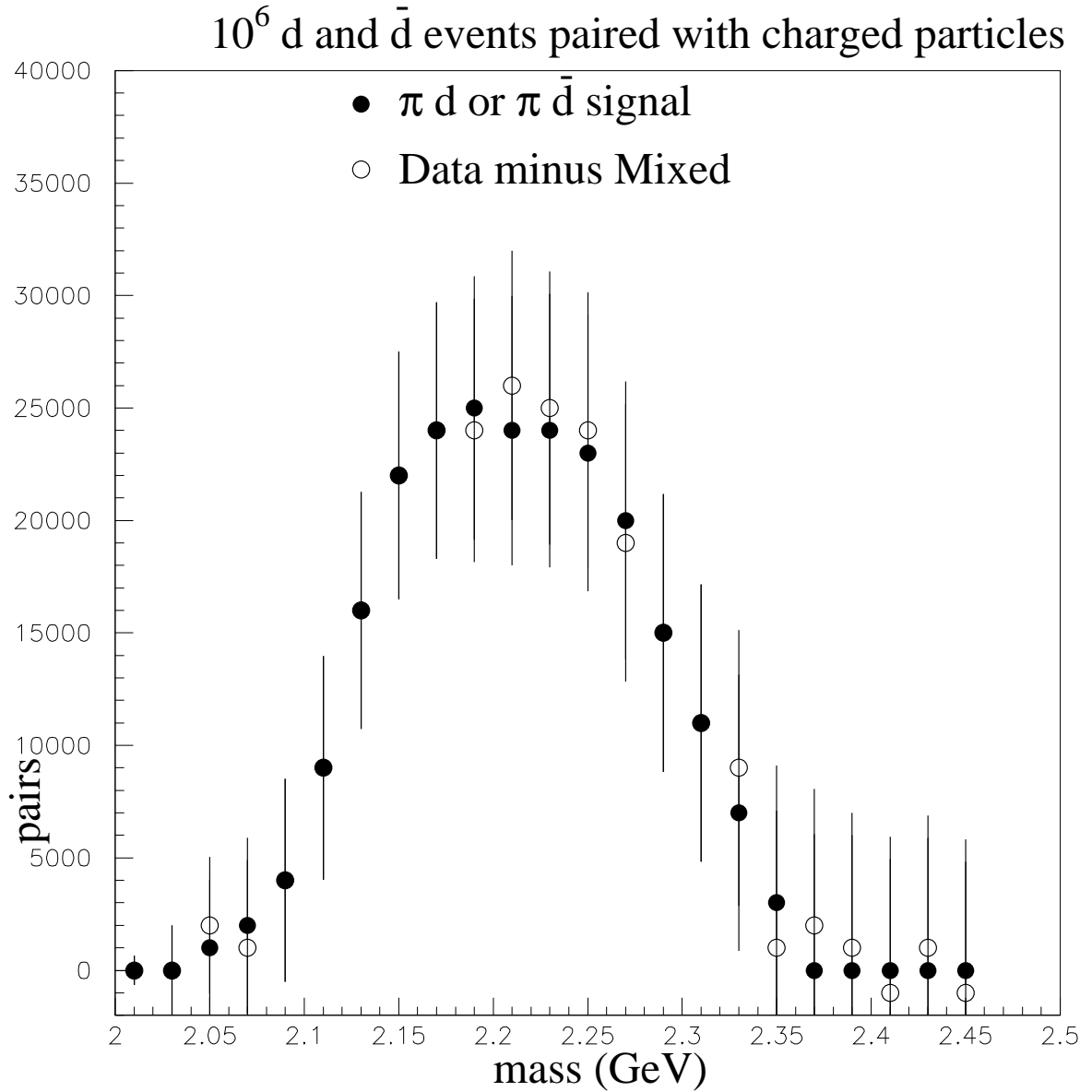


Figure 17: The number of d or \bar{d} paired with charged pions coming from 10^6 dibaryons decays within the STAR acceptance plotted as solid points. The open points are form by all d and \bar{d} paired with the charged particles in each event in the star acceptance minus the same d and \bar{d} paired with the charged particles from other events(mixed events).

We create a Monte Carlo simulation that should give realistic events structure with realistic dibaryon production. With the ability to measure hundreds of million ultra-relativistic heavy ion collisions, we predicted that a clear dibaryon signal decaying into $d\pi$ should be measured.

4 Acknowledgments

This research was supported by the U.S. Department of Energy under Contract No. DE-AC02-98CH10886.

References

- [1] T.A. Armstrong *et al.*, Phys. Rev. Lett. 83 (1999) 5431.
- [2] H. Agakishiev *et al.*, Nature 473 (2011) 353.
- [3] R.A. Arndt *et al.*, Phys. Rev. C 76 (2007) 025209.
- [4] C.H. Oh *et al.*, Phys. Rev. C 56 (1997) 635.
- [5] D. Schiff and J. Tran Thanh Van, Nucl. Phys. B5 (1968) 529.
- [6] R. Longacre, Phys. Rev. D 42 (1990) 874.
- [7] K. Geiger and R. Longacre, Heavy Ion Phys. 8 (1998) 41.